

Resonant microchannel volume and mass measurements show that suspended cells swell during mitosis

Sungmin Son,^{1,2*} Joon Ho Kang,^{1,3*} Seungeun Oh,⁵ Marc W. Kirschner,⁵ T.J. Mitchison,⁵ and Scott Manalis^{1,2,4}

¹Koch Institute for Integrative Cancer Research, Massachusetts Institute of Technology, Cambridge, MA 02142

²Department of Mechanical Engineering, ³Department of Physics, and ⁴Department of Biological Engineering, Massachusetts Institute of Technology, Cambridge, MA 02139

⁵Department of Systems Biology, Harvard Medical School, Boston, MA 02115

Osmotic regulation of intracellular water during mitosis is poorly understood because methods for monitoring relevant cellular physical properties with sufficient precision have been limited. Here we use a suspended microchannel resonator to monitor the volume and density of single cells in suspension with a precision of 1% and 0.03%, respectively. We find that for transformed murine lymphocytic leukemia and mouse pro-B cell lymphoid cell lines, mitotic cells reversibly increase their volume by more than 10% and decrease their density by 0.4% over a 20-min period. This response is correlated with the mitotic cell cycle but is not coupled to nuclear osmolytes released by nuclear envelope breakdown, chromatin condensation, or cytokinesis and does not result from endocytosis of the surrounding fluid. Inhibiting Na-H exchange eliminates the response. Although mitotic rounding of adherent cells is necessary for proper cell division, our observations that suspended cells undergo reversible swelling during mitosis suggest that regulation of intracellular water may be a more general component of mitosis than previously appreciated.

Introduction

Recent findings that regulation of intracellular hydrostatic pressure facilitates mitotic rounding of adherent cells highlight the mechanical role of osmotic forces in mitosis (Stewart et al., 2011). Forces generated by internal osmotic pressure can help cells within confined microenvironments round up, which is known to contribute to the fidelity of chromosome segregation (Lancaster et al., 2013; Cadart et al., 2014). On the other hand, whether and how osmotic regulation of cell volume affects mitosis is poorly understood. Previous studies in normal cells and cancer cells found that the activity of certain ion channels is coupled to mitosis, and cell proliferation is reduced when those ion channels are inhibited (Zheng et al., 2002; Habela and Sontheimer, 2007; Huang et al., 2012). It was predicted that the altered intracellular water content affects the length of mitosis by changing cell physicochemistry such as enzyme rates, signaling, and diffusion of macromolecules. These predictions assume that the osmotic regulation found in mitosis alters cell volume.

Quantitative measurement of a single cell's volume and water content has been challenging, especially during mitosis, when the cell changes its shape. Previous methods computed cell volume from confocal sections of cell boundary detected by the membrane or soluble dyes (Zheng et al., 2002; Habela and

Sontheimer, 2007; Boucrot and Kirchhausen, 2008). However, these methods are prone to error from variation in labeling or artifacts in volume reconstruction. In another approach, atomic force microscopy was used to uniaxially confine a cell so that its volume could be calculated based on diameter and shape (Stewart et al., 2011; Fischer-Friedrich et al., 2014). Although that method is more direct, it is possible that the mechanical constraints applied could alter cell volume. In this issue, Zlotek-Zlotkiewicz et al. use a fluorescence exclusion method together with quantitative phase microscopy to observe that volume reversibly increases by $\leq 30\%$, whereas dry mass remains constant during mitosis for a broad range of adherent and suspended cells.

In this study, we monitored the volume and density of single-suspension cells using a suspended microchannel resonator (SMR). We found that both transformed murine lymphocytic leukemia cell line L1210 and pro-B cell lymphoid cell line FL5.12 exhibited $>10\%$ volume increases during mitosis because of swelling. We demonstrate that the swelling and shrinking are closely associated with specific stages in mitosis, yet are not coupled to nuclear osmolytes released by nuclear envelope breakdown (NEB), chromatin condensation, or cytokinesis. Despite the rapid accumulation of endosomes known to occur in early M phase (Boucrot and Kirchhausen, 2007), we found that endosome accumulation is not the primary mechanism of swelling. Instead,

*S. Son and J.H. Kang contributed equally to this paper.

Correspondence to Scott Manalis: srm@mit.edu

S. Son's present address is Dept. of Bioengineering, University of California, Berkeley, Berkeley, CA 94720.

Abbreviations used in this paper: EIPA, ethylisopropylamide; NEB, nuclear envelope breakdown; SMR, suspended microchannel resonator; STLC, S-trityl-L-cysteine.

© 2015 Son et al. This article is distributed under the terms of an Attribution-Noncommercial-Share Alike-No Mirror Sites license for the first six months after the publication date (see <http://www.rupress.org/terms>). After six months it is available under a Creative Commons license [Attribution-Noncommercial-Share Alike 3.0 Unported license, as described at <http://creativecommons.org/licenses/by-nc-sa/3.0/>].

we show with an inhibition experiment that osmotic water exchange driven by activation of ion exchangers alters cell volume.

Results and discussion

Measurement of cell volume, mass, and density during mitosis using SMR

Instead of an optical approach, the SMR uses a mechanical principle to directly measure the buoyant mass of a single cell with extraordinary precision (Burg et al., 2007). When a cell that is lighter or denser than the surrounding fluid passes through the fluid channel embedded in the SMR, the net change in mass alters the resonant frequency, which is linearly proportional to the cell's buoyant mass and inherently independent of its shape (Fig. 1 A). We demonstrated that by measuring the buoyant mass of the same cell in two fluids of different densities, the volume, mass, and density of the cell could be obtained based on Archimedes' principle (Fig. 1 B; see Materials and methods; Grover et al., 2011). However, the complexity of fluid control involved in the two-fluid measurement previously limited measurements to only once per cell.

Here we combine a fluidic control method that enabled continuous measurement of the same cell (Son et al., 2012) with the two-fluid measurement to monitor cell volume, mass, and density throughout the cell cycle. In each measurement period (100 s), we kept the cell in the bypass channel containing normal medium for the majority of the time (80 s) and occasionally moved it through the SMR to dense medium (20 s), thereby minimizing shear stress as well as stress from the low nutrient levels in the dense medium (Fig. 1 A). The geometry of the fluid channels was designed to enhance the mixing of two fluids, which was critical for minimizing background noise. This, combined with the high-precision measurement of buoyant mass enabled by using the second vibration mode of the SMR (Fig. 1 A, inset; Lee et al., 2011), allowed the volume and density of an L1210 cell to be measured within 1% and 0.03%, respectively, throughout the cell cycle (Fig. S1). Based on the measurement of a cell's volume, mass, and density, we can observe the change of intracellular water content in nonisopycnic growth (Fig. 1 B).

Suspension cells reversibly alter internal water content at specific mitotic stages

Observation of cell volume, mass, and density with high precision and temporal resolution revealed the dynamic nature of water regulation that occurs throughout the cell cycle (Fig. 1 C) and most prominently during M phase (Fig. 1, C [inset] and D). L1210 and FL5.12 cells rapidly increased their volume by 12% and 11%, respectively, within 20 min during early mitosis and completely reversed the increase within 10 min before cell division (Fig. 1, D–F; and Fig. S2, A and B). In contrast to the large change in volume, the buoyant mass measured in normal medium remained constant, indicating that the volume increase is caused by a gain of water and not growth. The magnitude of swelling showed a weak correlation with volume at mitosis entry (Pearson correlation coefficient = 0.53), and its coefficient of variation remained within 0.24 for both cell types (Fig. 1 E), indicating the robustness of the process.

To determine whether swelling and shrinking are associated with specific stages in mitosis, we used cell-cycle drugs

to arrest mitosis in various stages while monitoring a cell's volume (Fig. 2). We performed confocal imaging of L1210 cells that stably express fluorescently tagged geminin (geminin-mAG) to validate that a given drug arrested the cells at the expected cell-cycle position and that the cells remained healthy during treatment. Geminin is present only from S to early M phases, and we observe that upon NEB, it diffuses from the cell nucleus to the cytoplasm. When combined with chromosome imaging and cell shape, this information enabled us to discern the mitotic cell population for each drug (Fig. 2, A and B). We then measured the single-cell mass, volume, and density response after drug treatment. When we arrested a cell at the ATR-mediated G_2 checkpoint using topoisomerase II catalytic inhibitor ICRF-193 (Deming et al., 2002), it continuously grew without showing any swelling and became significantly larger than the mean size at mitosis (Figs. 2 D S2 C). Next, when we arrested a cell in metaphase using the kinesin inhibitor *S*-trityl-L-cysteine (STLC) or the microtubule inhibitor nocodazole, the cell exhibited swelling but did not shrink (Fig. 2 E; Fig. S2, D and E; and Fig. S3). Finally, when we inhibited cytokinesis using the myosin II inhibitor blebbistatin, mitotic cells proceeded through both swelling and shrinking but remained spherical in the absence of cytokinesis (Figs. 2 F and S2 F). These observations unambiguously reveal that cells swell during prophase and pro-metaphase and shrink during anaphase and telophase and that the swelling is not dependent on cytokinesis.

Mitotic swelling is not linked to chromatin condensation or passive diffusion of nuclear osmolytes released by NEB

We sought to determine whether mitotic swelling is coupled to a specific event during mitosis. Given the rapid rate of swelling, it seems plausible that release of osmolytes within the nucleus upon NEB increases cytosolic osmolarity and, in turn, a cell's volume. If swelling is indeed driven by the passive diffusion of nuclear osmolytes, then the duration of swelling should be independent of the length of mitosis, because NEB is a discrete process. However, when we treated a cell with a low dose of Cdk1 inhibitor RO-3306, which slows down the entry of mitosis, the duration of swelling was significantly extended (Fig. 3, A–C; and Fig. S2 G). Alternatively, we postulated that mitotic swelling is associated with chromatin condensation. To test this, we used ICRF-193 along with caffeine to perturb chromatin condensation while the G_2 –M transition remained unchecked. Cells treated with ICRF-193 showed extended metaphase similar to cells treated with nocodazole or STLC, consistent with previous findings that reduced chromatin condensation can lead to delayed chromosome segregation (Fig. 3, D and E; and Fig. S2 H; Baxter and Aragón, 2012). However, cells treated with ICRF-193 showed a larger magnitude of swelling despite reduced chromosome condensation (Fig. 3 F). These observations suggest that mitotic swelling is not directly coupled to NEB or chromatin condensation, even though these independent events occur concurrently during normal mitosis.

Mitotic swelling is driven by osmotic water exchange and not by endocytosis

It has been suggested that osmotic regulation of hydrostatic pressure during mitosis of adherent cells requires active ion

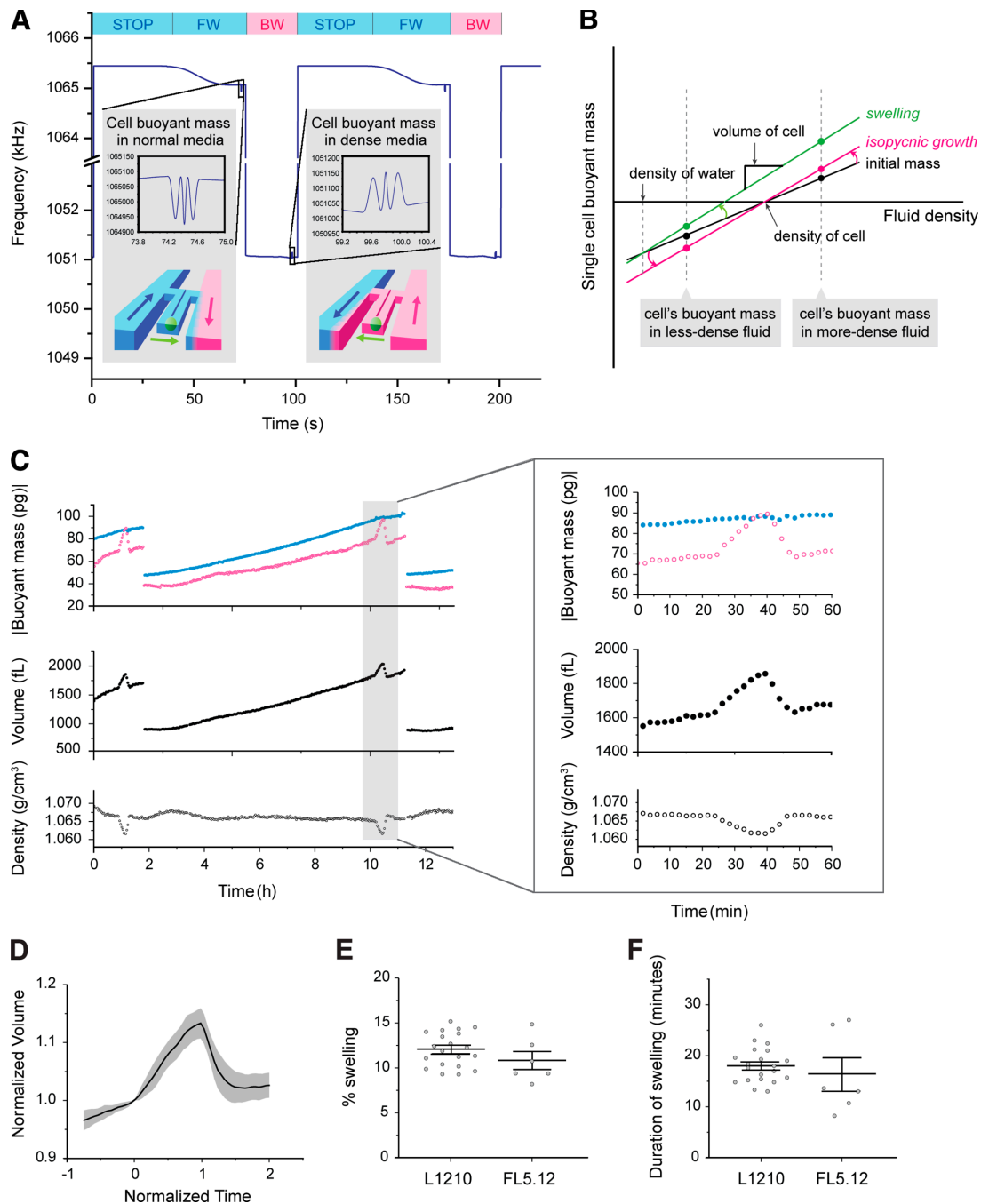


Figure 1. Measurement of cell volume, mass, and density during mitosis. (A) Frequency of the SMR during the measurement of a cell's buoyant mass in two different fluids. The color bars and the illustration of the SMR in the inset indicate the fluid surrounding a cell and the direction of its flow within the SMR (blue, normal medium; magenta, dense medium; FW, forward flow; BW, backward flow). Insets show the shift in SMR frequency upon the passage of the cell. Cell buoyant mass was determined by the height of the two side peaks (see SMR in Materials and methods). (B) Mass, volume, and density can be determined by weighing a cell in two fluids of different density and plotting the linear relationship between buoyant mass and fluid density. For isopycnic growth (from black line to magenta line), the absolute value of buoyant mass increases proportionally. For swelling (from black line to green line), the buoyant mass in the dense medium significantly increases, whereas the buoyant mass in the normal medium remains almost constant. (C) Buoyant mass measured in normal and dense medium and the resulting volume and density of the same cell measured over the complete cell cycle and during mitosis (inset). After division, only one of the daughter cells is retained in the flow trap. (D) Mean trajectory of L1210 cell volume during mitosis. Volume is normalized by the volume at the onset of swelling. The gray area indicates SD. The time is aligned such that the swelling starts at 0 and ends at 1. $n = 20$. See Fig. S2 A for single-cell data. (E) Magnitude of swelling during mitosis of L1210 ($n = 20$, SEM = 0.42) and FL5.12 ($n = 6$, SEM = 0.92) cells. (F) Duration of swelling during mitosis of L1210 ($n = 20$, SEM = 0.75) and FL5.12 ($n = 6$, SEM = 3.0) cells. See Fig. S2 B for single-cell data.

exchange (Stewart et al., 2011). To investigate whether the water regulation in mitosis of cells in suspension and adherent cells share the same mechanism, we tested the effect of ion exchangers and endocytosis on mitotic swelling. Among

many ion exchangers, the Na-H exchanger is regulated by the RhoA pathway (Hooley et al., 1996), which is activated at mitosis entry. Furthermore, the Na-H exchanger is known to play a critical role in regulatory volume increase after hypertonic

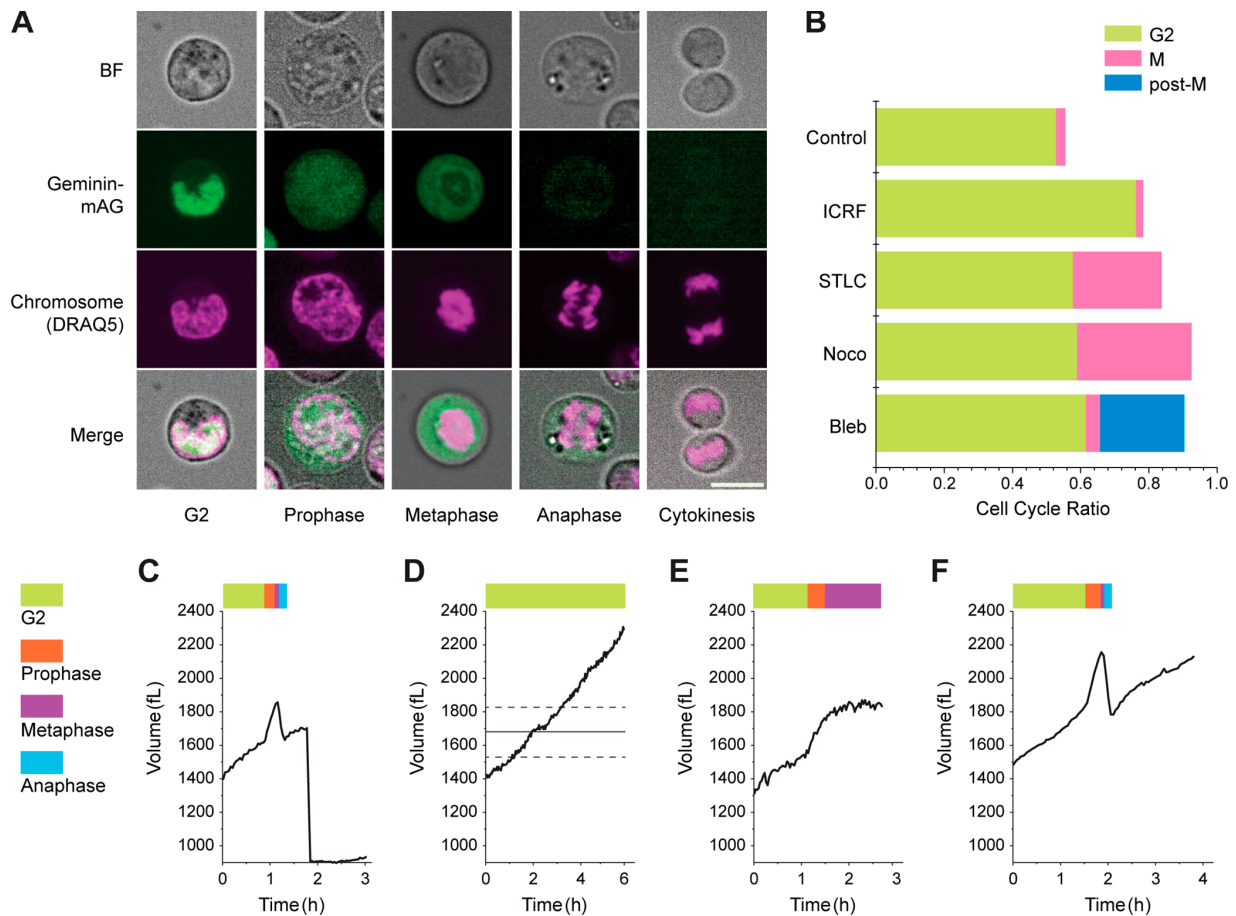


Figure 2. Alteration of cell volume is associated with specific mitotic stages. (A) Confocal images of L1210 cells are used to validate drug-induced arrest in G₂ or mitosis. Cell-cycle position is determined based on the localization of geminin-mAG, chromatin condensation, and cell shape. BF, bright field. Bar, 10 μ m. (B) Proportion of L1210 cells in G₂ or mitosis 6 h after treatment with various drugs. Cells showing geminin in the nucleus and diffused chromosome are in G₂ phase; cells showing geminin in the cytoplasm and condensed chromosome are in M phase. The large cells showing diffused chromosome but no geminin are post-M phase. Number of cells measured for DMSO control, 641; 20 ng/ml ICRF, 550; 5 μ M STLC, 553; 1 μ g/ml nocodazole, 417; and 20 μ M blebbistatin, 357. (C) Volume trajectory of a control L1210 cell. (D) L1210 cell treated with 20 ng/ml ICRF-193. The straight line and the dotted lines indicate the mean and SD of cell volume upon mitosis entry based on 20 L1210 cells shown in Fig. 1 D (see Fig. S2 C for single-cell data). (E) Cell treated with 5 μ M STLC (see Fig. S2 [D and E] for single-cell data). (F) Cell treated with 20 μ M blebbistatin (see Fig. S2 E for single-cell data).

shrinkage (Alexander and Grinstein, 2006). We therefore hypothesized that it may be associated with autonomous cell volume increase during mitosis. Indeed, when the Na-H exchanger was inhibited using ethylisopropylamiloride (EIPA), the amount of swelling was significantly reduced (Fig. 4, A and B; and Fig. S2 I). Alternatively, we wondered whether the rapid accumulation of endosomes known to occur in early M phase (Boucrot and Kirchhausen, 2007) contributes to mitotic swelling. To test this, we exploited the fact that the buoyant mass change reflects only an exchange of material that is either heavier or lighter than the surrounding fluid. We measured the buoyant mass of an L1210 cell in dense medium only (without switching to normal medium). If swelling were caused by endocytosis of the surrounding fluid, then the buoyant mass would be expected to remain constant (Fig. 4 C). However, the buoyant mass measurement revealed a trajectory similar to that obtained by the fluidic switching method, in which the cell was exposed to dense medium for only ~10% of the time (Fig. 4 D). This result suggests that endocytosis is not the primary mechanism for cell swelling.

In this issue, we and Zlotek-Zlotkiewics et al. (2015) present independent methods for monitoring single-cell volume and water content and show that mitotic swelling is conserved

between adherent cells and cells in suspension. Despite ample evidence that osmotic regulation is critical for mitosis and cell proliferation (Zimmerman, 1993), the mechanism by which osmotic regulation influences mitosis is poorly understood. Recent findings that cell rounding is indispensable for efficient chromosome segregation (Lancaster et al., 2013; Cadart et al., 2014) support the idea that osmoregulation provides mechanical force to deform the surrounding microenvironment during cell rounding (Stewart et al., 2011; Fischer-Friedrich et al., 2014). However, an equally important aspect of osmotic regulation—alterations in cell volume and density—has been unresolved because of a lack of precise measurement of mitotic cell size. Some studies observed cell volume decrease before mitosis in BSC1 monkey kidney epithelial cells and D54-MG glioma cells, and it was argued that the concentrated cytoplasm can promote mitosis by accelerating mitotic signaling through a molecular crowding effect (Habela and Sontheimer, 2007; Boucrot and Kirchhausen, 2008). Yet conflicting observations of cell volume increase and swelling during mitosis have been made in HeLa cells and rat pancreatic acinar cells (Wolff and Pertoft, 1972; Abrahamsohn and Sesso, 1983). Also, others found that cell division depended on increased cell volume (Lang et al., 1998).

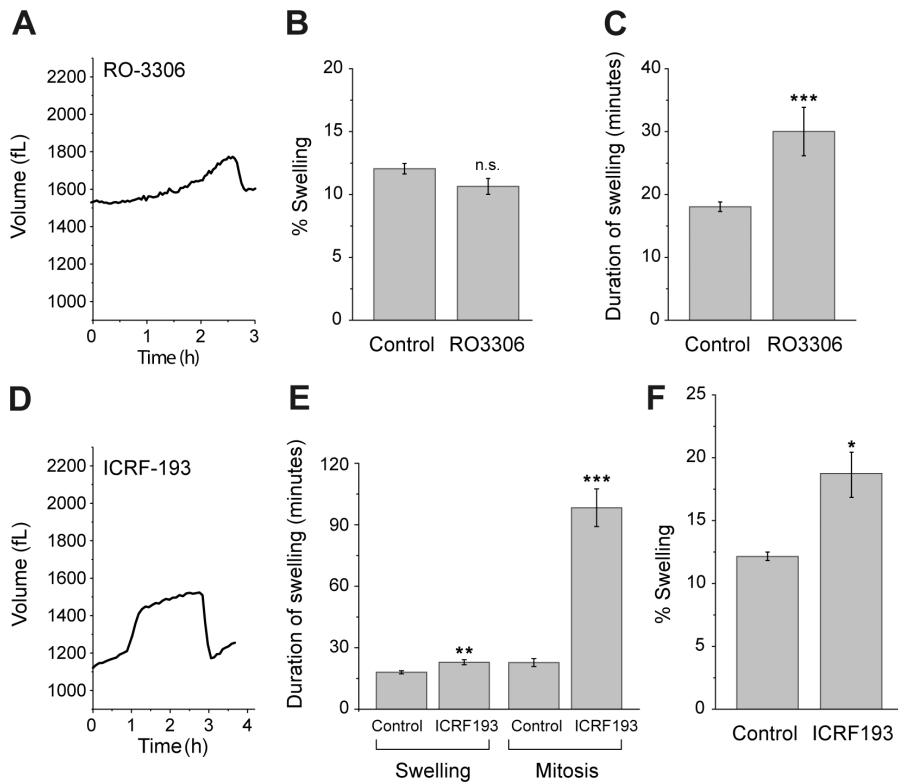


Figure 3. Mitotic swelling is not directly coupled to NEB or chromatin condensation. (A) L1210 cell treated with 2 μ M RO-3306 (see Fig. S2 G for single-cell data). (B) Magnitude of swelling during mitosis of control L1210 cells ($n = 20$, SEM = 0.42) and L1210 cells treated with RO-3306 ($n = 11$, SEM = 0.63, $P = 0.074$). n.s., not significant. (C) Duration of swelling during mitosis of control L1210 cells ($n = 20$, SEM = 2.3) and L1210 cells treated with RO-3306 ($n = 11$, SEM = 3.85, ***, $P < 0.001$). (D) L1210 cell treated with both 20 ng/ml ICRF-193 and 5 mM caffeine (see Fig. S2 H for single-cell data). (E) Duration of either swelling or the entire mitosis of control L1210 cells ($n = 20$, SEM = 0.75 and 2.30) and L1210 cells treated with 10 μ g/ml ICRF-193 and 5 mM caffeine ($n = 10$, SEM = 1.21 and 9.17); **, $P = 0.0014$; ***, $P < 0.001$. (F) Magnitude of swelling during mitosis of control L1210 cells and L1210 cells treated with ICRF-193 and caffeine ($n = 10$, SEM = 0.83; *, $P = 0.018$). P-values were calculated with Welch t test.

Although part of the discrepancy may be attributed to differences in cell types, the consistent observation of mitotic swelling by Zlotek-Zlotkiewicz et al. (2015) and us in both adherent and suspension cells suggests that it is a conserved element of mitotic events with physiological roles. A larger space created by swelling may assist the rigorous and fast rearrangement of chromosomes during mitosis (Magidson et al., 2011), or the diluted state of cytoplasm may facilitate the movement of

large macromolecules such as chromosome and microtubules, as well as organelles such as Golgi and mitochondria, which become fragmented during mitosis (Kashatus et al., 2011; Yamano and Youle, 2011; Yadav et al., 2012). Cell swelling may function as part of a mitosis signaling pathway, similarly to the way cell volume increase evokes a range of downstream responses in transepithelial transport, cell migration, and proliferation (Hoffmann et al., 2009). Also, decrowding of the

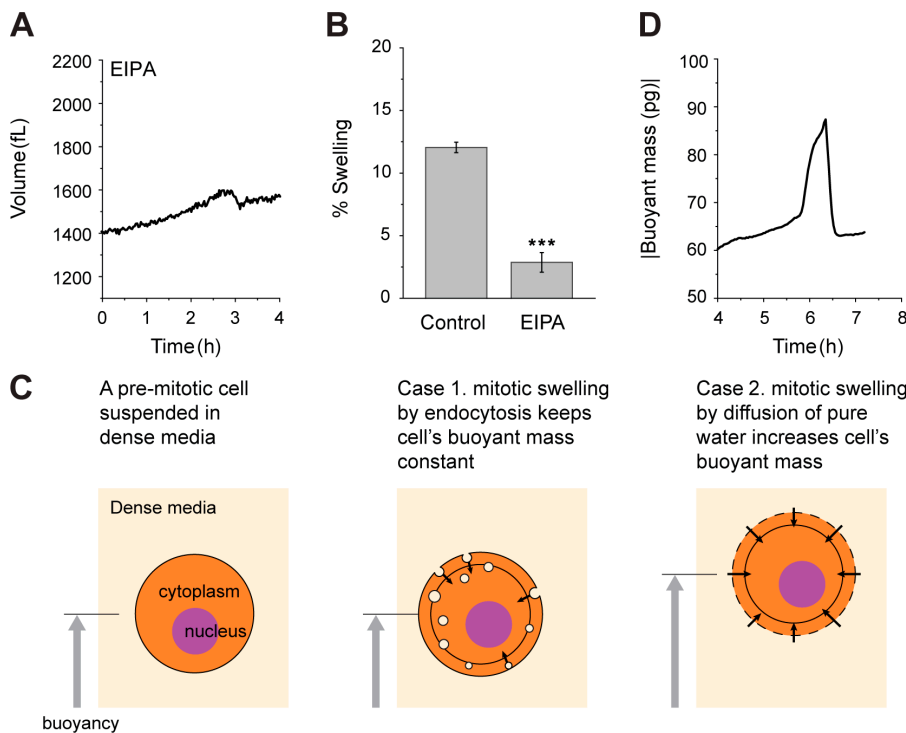


Figure 4. Mitotic swelling is driven by osmotic water exchange and not by endocytosis. (A) L1210 cell treated with 5 μ M EIPA (see Fig. S2 I for single-cell data). (B) Control L1210 cells ($n = 20$, SEM = 0.42) and L1210 cells treated with EIPA ($n = 8$, SEM = 0.79; ***, $P < 0.001$). Because the time when cells start to swell is difficult to discern for cells treated with EIPA, the magnitude of shrinking was used instead of swelling. (C) Schematics illustrating two hypotheses of mitotic swelling. When a premitotic cell is suspended in dense medium (light blue), it maintains positive buoyant mass. If a cell swells by internalizing endosomes (light blue circles in the cell), then the buoyant mass remains constant because the internalized medium has the same density as the surrounding medium. If a cell swells by taking up water, its buoyant mass will increase. The gray circle indicates the original cell size before swelling. (D) Buoyant mass of a L1210 cell during mitosis measured only in the dense medium.

cytoplasm may directly affect the interaction of macromolecules (Zimmerman, 1993). Such a global change of biochemical activity is not implausible in mitotic cell physiology, considering the finding that transcription and translation stop during mitosis (Mitchison, 2003).

Materials and methods

SMR

The principles behind the SMR have been described (Burg et al., 2007). In brief, cells in suspension are transported through the SMR, resulting in a transient shift in resonant frequency. When resonating in the second vibration mode, the SMR generates three peaks as the cell passes through the channel (Lee et al., 2011). The magnitude of the two side peaks is identical and independent of the flow path that a cell takes within the SMR, allowing the buoyant mass to be measured with a precision of 0.8% in normal medium and 1.5% in dense medium (Fig. S1). For the two-fluid switching measurement, dense medium was obtained by adding 30% Opti-Prep (60% iodixanol in water with a density of 1.32 g/ml) to RPMI medium to achieve a density of 1.10 g/ml. Because Opti-Prep is isosmotic, the osmolarity of the dense medium was identical to that of the normal medium. Based on the buoyant mass of a cell measured in two fluids of different density, the volume, mass, and density can be calculated by the following formula:

$$m_b = m_c \left(1 - \frac{\rho_f}{\rho_c} \right),$$

where m_b is the buoyant mass, m_c is the absolute mass, ρ_c is the density of a cell, and ρ_f is the fluid density. To measure a cell during mitosis, only cells larger than a certain size were selected and measured until division. Fluidic control was automated using Labview (National Instruments).

Cell culture and drugs

L1210 and FL5.12 cells were maintained in Leibovitz L-15 medium (Life Technologies) and RPMI medium (Invitrogen), respectively, supplemented with 10% FBS (Life Technologies) and 1% penicillin-streptomycin (Life Technologies). For the small-molecule drug experiments, cells were pretreated in a microwell plate and loaded in the SMR containing the drug. Drug concentrations used were ICRF-193 at 20 ng/ml (for G₂ arrest) or 10 μg/ml (for inhibition of chromatin condensation), 5 mM caffeine, 1 μg/ml nocodazole, 5 μM STLC, 20 μM blebbistatin, 2 μM RO-3306, and 5 μM EIPA. To determine whether the drugs tested can induce swelling regardless of mitosis, we measured the volume of L1210 cells with a Coulter Counter after 1 h of drug treatment and did not observe a significant increase in median cell volume (Fig. S3 C).

Imaging and image processing

L1210 cells that stably express geminin-mAG and Cdt1-mKO2 were imaged with a confocal microscope (Eclipse Ti-U; Nikon) using a spinning disk confocal (CSU-10; Yokogawa) and sCMOS camera (Zyla; Andor). Images were acquired using a 60× objective (CFI Apo TIRF, 1.49 NA, oil; Nikon) and analyzed using ImageJ (National Institute of Science). For the drug experiment, cells were treated for 5 h in a 96-well plate and transferred to a glass-bottom dish (Lab-Tek) 1 h before imaging. All the imaging was done at RT. 1 μM live-cell nuclear dye (DRAQ5; Abcam) was added 30 min before imaging. Expression levels of geminin-mAG and Cdt1-mKO2 were determined by integrating their fluorescent intensity within a cell. Cell cycle was determined by comparing the intensities of geminin-mAG and Cdt1-mKO2 within each cell (Sakaue-Sawano et al., 2008).

Data processing

To convert SMR frequency shift to buoyant mass, size-standard polystyrene beads (Bangs Lab) were measured. The buoyant mass, volume, and density trajectories were presented without any filtering. The beginning and end of the swelling and shrinking were detected based on a point-by-point derivative of the cell volume trajectory.

Online supplemental material

Fig. S1 shows the measurement error of the SMR in buoyant mass, volume, and density. Fig. S2 shows the single-cell volume trajectory of normal or drug-treated cells during mitosis. Fig. S3 shows mitotic swelling of L1210 cells treated with nocodazole and STLC and the volume of L1210 cells treated with various drugs measured using the Coulter Counter. Online supplemental material is available at <http://www.jcb.org/cgi/content/full/jcb.201505058/DC1>.

Acknowledgments

The authors thank Martin Stewart and Matthieu Piel for insightful comments.

We acknowledge support from the Physical Sciences Oncology Center U54CA143874 and the Koch Institute Support (core) grant P30-CA14051 from the National Cancer Institute. J.H. Kang acknowledges support through a Samsung Scholarship.

The authors declare no competing financial interests.

Submitted: 12 May 2015

Accepted: 1 October 2015

References

- Abrahamsohn, P.A., and A. Sesso. 1983. Volume changes during mitosis in pancreatic acinar cells of the rat. *Acta Anat. (Basel)*. 117:225–230. <http://dx.doi.org/10.1159/000145791>
- Alexander, R.T., and S. Grinstein. 2006. Na⁺/H⁺ exchangers and the regulation of volume. *Acta Physiol. (Oxf.)*. 187:159–167. <http://dx.doi.org/10.1111/j.1748-1716.2006.01558.x>
- Baxter, J., and L. Aragón. 2012. A model for chromosome condensation based on the interplay between condensin and topoisomerase II. *Trends Genet.* 28:110–117. <http://dx.doi.org/10.1016/j.tig.2011.11.004>
- Boucrot, E., and T. Kirchhausen. 2007. Endosomal recycling controls plasma membrane area during mitosis. *Proc. Natl. Acad. Sci. USA*. 104:7939–7944. <http://dx.doi.org/10.1073/pnas.0702511104>
- Boucrot, E., and T. Kirchhausen. 2008. Mammalian cells change volume during mitosis. *PLoS One*. 3:e1477. <http://dx.doi.org/10.1371/journal.pone.0001477>
- Burg, T.P., M. Godin, S.M. Knudsen, W. Shen, G. Carlson, J.S. Foster, K. Babcock, and S.R. Manalis. 2007. Weighing of biomolecules, single cells and single nanoparticles in fluid. *Nature*. 446:1066–1069. <http://dx.doi.org/10.1038/nature05741>
- Cadart, C., E. Zlotek-Zlotkiewicz, M. Le Berre, M. Piel, and H.K. Matthews. 2014. Exploring the function of cell shape and size during mitosis. *Dev. Cell*. 29:159–169. <http://dx.doi.org/10.1016/j.devcel.2014.04.009>
- Deming, P.B., K.G. Flores, C.S. Downes, R.S. Paules, and W.K. Kaufmann. 2002. ATR enforces the topoisomerase II-dependent G2 checkpoint through inhibition of Plk1 kinase. *J. Biol. Chem.* 277:36832–36838. <http://dx.doi.org/10.1074/jbc.M206109200>
- Fischer-Friedrich, E., A.A. Hyman, F. Jülicher, D.J. Müller, and J. Helenius. 2014. Quantification of surface tension and internal pressure generated by single mitotic cells. *Sci. Rep.* 4:6213. <http://dx.doi.org/10.1038/srep06213>
- Grover, W.H., A.K. Bryan, M. Diez-Silva, S. Suresh, J.M. Higgins, and S.R. Manalis. 2011. Measuring single-cell density. *Proc. Natl. Acad. Sci. USA*. 108:10992–10996. <http://dx.doi.org/10.1073/pnas.1104651108>
- Habela, C.W., and H. Sontheimer. 2007. Cytoplasmic volume condensation is an integral part of mitosis. *Cell Cycle*. 6:1613–1620. <http://dx.doi.org/10.4161/cc.6.13.4357>

- Hoffmann, E.K., I.H. Lambert, and S.F. Pedersen. 2009. Physiology of cell volume regulation in vertebrates. *Physiol. Rev.* 89:193–277. <http://dx.doi.org/10.1152/physrev.00037.200719126758>
- Hooley, R., C.-Y. Yu, M. Symons, and D.L. Barber. 1996. G alpha 13 stimulates Na⁺-H⁺ exchange through distinct Cdc42-dependent and RhoA-dependent pathways. *J. Biol. Chem.* 271:6152–6158. <http://dx.doi.org/10.1074/jbc.271.11.6152>
- Huang, X., A.M. Dubuc, R. Hashizume, J. Berg, Y. He, J. Wang, C. Chiang, M.K. Cooper, P.A. Northcott, M.D. Taylor, et al. 2012. Voltage-gated potassium channel EAG2 controls mitotic entry and tumor growth in medulloblastoma via regulating cell volume dynamics. *Genes Dev.* 26:1780–1796. <http://dx.doi.org/10.1101/gad.193789.112>
- Kashatus, D.F., K.-H. Lim, D.C. Brady, N.L.K. Pershing, A.D. Cox, and C.M. Counter. 2011. RALA and RALBP1 regulate mitochondrial fission at mitosis. *Nat. Cell Biol.* 13:1108–1115. <http://dx.doi.org/10.1038/ncb2310>
- Lancaster, O.M., M. Le Berre, A. Dimitracopoulos, D. Bonazzi, E. Zlotek-Zlotkiewicz, R. Picone, T. Duke, M. Piel, and B. Baum. 2013. Mitotic rounding alters cell geometry to ensure efficient bipolar spindle formation. *Dev. Cell.* 25:270–283. <http://dx.doi.org/10.1016/j.devcel.2013.03.014>
- Lang, F., G.L. Busch, M. Ritter, H. Völkl, S. Waldegger, E. Gulbins, and D. Häussinger. 1998. Functional significance of cell volume regulatory mechanisms. *Physiol. Rev.* 78:247–306.
- Lee, J., A.K. Bryan, and S.R. Manalis. 2011. High precision particle mass sensing using microchannel resonators in the second vibration mode. *Rev. Sci. Instrum.* 82:023704. <http://dx.doi.org/10.1063/1.3534825>
- Magidson, V., C.B. O'Connell, J. Lončarek, R. Paul, A. Mogilner, and A. Khodjakov. 2011. The spatial arrangement of chromosomes during prometaphase facilitates spindle assembly. *Cell.* 146:555–567. <http://dx.doi.org/10.1016/j.cell.2011.07.012>
- Mitchison, J.M. 2003. Growth during the cell cycle. *Int. Rev. Cytol.* 226:165–258. [http://dx.doi.org/10.1016/S0074-7696\(03\)01004-0](http://dx.doi.org/10.1016/S0074-7696(03)01004-0)
- Sakaue-Sawano, A., H. Kurokawa, T. Morimura, A. Hanyu, H. Hama, H. Osawa, S. Kashiwagi, K. Fukami, T. Miyata, H. Miyoshi, et al. 2008. Visualizing spatiotemporal dynamics of multicellular cell-cycle progression. *Cell.* 132:487–498. <http://dx.doi.org/10.1016/j.cell.2007.12.033>
- Son, S., A. Tzur, Y. Weng, P. Jorgensen, J. Kim, M.W. Kirschner, and S.R. Manalis. 2012. Direct observation of mammalian cell growth and size regulation. *Nat. Methods.* 9:910–912. <http://dx.doi.org/10.1038/nmeth.2133>
- Stewart, M.P., J. Helenius, Y. Toyoda, S.P. Ramanathan, D.J. Muller, and A.A. Hyman. 2011. Hydrostatic pressure and the actomyosin cortex drive mitotic cell rounding. *Nature.* 469:226–230. <http://dx.doi.org/10.1038/nature09642>
- Wolff, D.A., and H. Pertoft. 1972. Separation of HeLa cells by colloidal silica density gradient centrifugation. I. Separation and partial synchrony of mitotic cells. *J. Cell Biol.* 55:579–585. <http://dx.doi.org/10.1083/jcb.55.3.579>
- Yadav, S., M.A. Puthenveedu, and A.D. Linstedt. 2012. Golgin160 recruits the dynein motor to position the Golgi apparatus. *Dev. Cell.* 23:153–165. <http://dx.doi.org/10.1016/j.devcel.2012.05.023>
- Yamano, K., and R.J. Youle. 2011. Coupling mitochondrial and cell division. *Nat. Cell Biol.* 13:1026–1027. <http://dx.doi.org/10.1038/ncb2334>
- Zheng, Y.-J., T. Furukawa, T. Ogura, K. Tajimi, and N. Inagaki. 2002. M phase-specific expression and phosphorylation-dependent ubiquitination of the CIC-2 channel. *J. Biol. Chem.* 277:32268–32273. <http://dx.doi.org/10.1074/jbc.M202105200>
- Zimmerman, S.B. 1993. Macromolecular crowding effects on macromolecular interactions: some implications for genome structure and function. *Biochim. Biophys. Acta.* 1216:175–185. [http://dx.doi.org/10.1016/0167-4781\(93\)90142-Z](http://dx.doi.org/10.1016/0167-4781(93)90142-Z)
- Zlotek-Zlotkiewicz, E., S. Monnier, G. Cappello, M. Le Berre, and M. Piel. 2015. Optical volume and mass measurements show that mammalian cells swell during mitosis. *J. Cell Biol.* <http://dx.doi.org/10.1083/jcb.201505056>